TRIBHUVAN UNIVERSITY

INSTITUTE OF

ENGINEERINGPULCHOWK

CAMPUS

THESIS NO: S020/075

Fatigue Life Analysis of Steel-Concrete Composite Bridge Considering Road Surface Condition

by

Utkarsha Bhetuwal

A THESIS
SUBMITTED TO THE DEPARTMENT OF CIVIL ENGINEERING
IN PARTIAL FULFILLMENT OF THE REQUIREMENTS FOR
THE
DEGREE OF MASTER OF SCIENCE IN
STRUCTURAL ENGINEERING

DEPARTMENT OF CIVIL
ENGINEERINGLALITPUR, NEPAL

SEPTEMBER, 2021

COPYRIGHT

CERTIFICATON OF APPROVAL

TRIBHUVAN UNIVERSITY

INSTITUTE OF ENGINEERING

DEPARTMENT OF CIVIL ENGINEERING

PULCHOWK CAMPUS

The undersigned certify that he/she has read, recommended to the Institute of Engineering for acceptance, a thesis entitled, "**Fatigue Life Analysis of Steel-Concrete Composite Bridge Considering Road Surface Condition**" submitted by Utkarsha Bhetuwal (075/MSStE/20) in partial fulfillment of requirement for the degree of Master of Science in Structural Engineering.

Supervisor,
Asso. Prof. Dr. Jagat Kumar Shrestha,
Department of Civil Engineering,
Institute of Engineering
Pulchowk Campus

External Supervisor,
Dr. Bijaya Jaishi
Director,
Quality, Research and Development Center
Department of Roads

Program Coordinator, Assoc. Prof. Dr. Kamal Bahadur Thapa
Department of Civil Engineering
Institute of Engineering
Pulchowk Campus

ABSTRACT

The road surface roughness affects the dynamic interaction between vehicle. Due to this, the dynamic impact in the bridge due to vehicle is more if the road surface condition in the bridge is poor. This thesis presents a detailed analysis of a composite steel-concrete bridge for its fatigue life with inclusion of road surface condition. The model takes in to account the dynamic impact of vehicle on bridge and the stresses induced in the bridge girder affected by road surface condition in the bridge deck. The Finite Element Modeling of both vehicle and bridge is done in ANSYS- APDL and vehicle bridge interaction analysis is carried out. The results are presented to show the effect of good, average and poor road surface condition on the bridge's fatigue life. It is found that the bridge with poor road surface condition has low fatigue life in compared to bridge with good road surface condition. The fatigue life is calculated using Linear Elastic Fracture Mechanics (LEFM) approach which considers crack size information. This study can also be applied for the bridge with existing crack, of which, remaining fatigue life can be computed.

ACKNOWLEDGEMENT

Foremost, I would like to express my sincere gratitude to my respected supervisor Asso. Prof. Jagat Kumar Shrestha for continuous support and motivation throughout my research work. His helpful guidance and valuable suggestion made me work harder than I ever could.

I would also like to acknowledge all the faculty members of Department of Civil Engineering for the knowledge and concepts they gave me during my study at IOE, Pulchowk Campus.

I am thankful to Roads Board Nepal for providing financial supports to conduct this work. Also, I am thankful to Center for Infrastructure Development Studies (CIDS) for providing technical support and knowledge for completion of this study.

Finally, I wish to thank my family who encouraged me every day to keep on striving towards my goal. Their words of support gave the much-needed motivation to persevere in the hardest of times.

TABLE OF CONTENTS

List of Symbols

a	Crack Depth
ANSYS	Analaysis Systems
APDL	Ansys Parametric Design Language
c	Half crack length
FEM	Finite Element Menthod
m and C	Crack growth constants
MATLAB	Matrix Laboratory
MDOF	Multi- Degree of Freedom
n	Spatial Frequency
N	Number of cycle before fatigue failure
PSD	Power Spectral Density
q_i	Generalized Coordinates
SIMULINK	simulating and analyzing multidomain dynamical systems
T	Kinetic Energy of System
V	Potential Energy of System
α	Mass proportional constant for Rayleigh Damping
β	Stiffness proportional constant for Rayleigh Damping
$\Delta\sigma$	Stress Range
ξ	Damping Ratio
ω	Natural Frequency of Bridge

List of Figures

List of Tables

CHAPTER 1: INTRODUCTION

1.1 Background of study

Fatigue is the type of failure of material when the material is subjected to cyclic stress. If there is presence of inherent crack in the structural steel (due to weld defect, construction stress, stress concentration or by any means as shown in Fig: 1.1), the cyclic stress causes the crack to propagate with time until fracture of material occurs. The structural components of the bridge are subjected to cyclic stress due to different traffic loads hence are prone to fatigue failure. Although steel has very high yield strength, stress value way below the yield strength, if applied repeatedly, causes brittle failure. Fatigue life analyisis, which is defined as predicting remaining number of load cycles of load that can be applied in bridge before fatigue failure, is hence essential both for design of new bridge and maintenance of existing bridge.

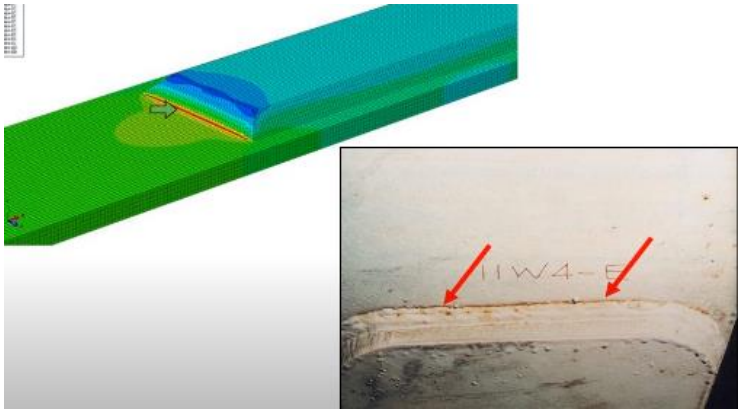

Fig: 1.1 Stress Concentration at bridge detail (flange and cover plate connection)

The stresses are produced due to the dynamic interaction between vehicle and bridge. The road surface above the decking of the bridge deteriorates with time which affects dynamic interaction between vehicle and bridge. Same vehicle can produce different stress values in the bridge girder if the road surface condition above the decking slab is different. So, it is important to consider the road surface profile to analyze the fatigue life of the bridge because different road condition gives rise to different fatigue life of bridge.

There are many methods for analyzing the fatigue performance of the bridge. The most popular method is the method given by the American Association of State Highway and Transportation Officials (AASHTO) - Load and Resistance Factor Design (LRFD) design specifications. Another method of analysis is through fracture mechanics approach. Under fracture mechanics approach, there are two methods; they are Linear Elastic Fracture

Mechanics (LEFM) and Elasto-Plastic Fracture Mechanics (EPFM). This research, however, is focused on LEFM method. The reasons for choosing LEFM approach over AASHTO method and EPFM method will be discussed in upcoming sections.

1.2 Problem Statement

AASHTO proposes S-N curve approach that contains curves relating Stress Range (S) and the number of cycles to failure (N) due to fatigue. The SN curve provided by AASHTO is shown in Fig: 1.2. These are design fatigue curves constructed experimentally. These curves, however, combine artificially high-stress range with an artificially low number of cycles to produce a reasonable design. Hence this method is more useful for the design of new bridges. Also, this method does not give information about crack size and its growth.

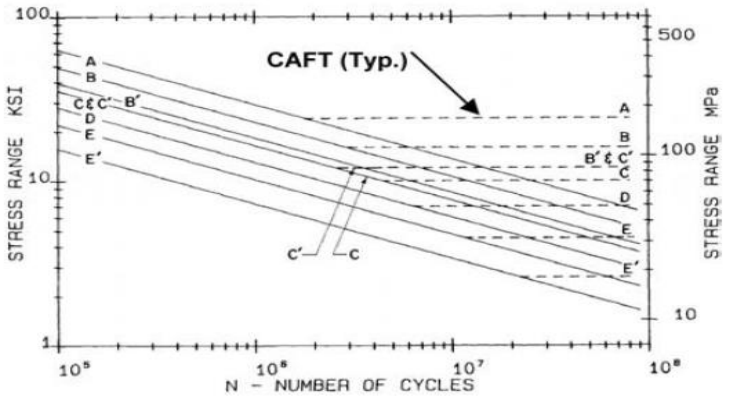

Fig: 1.2 AASHTO S-N curve

Another approach, which is already introduced earlier, is fracture mechanics approach. Fracture mechanics deals with propagation of crack in the material. If the material with inherent crack is loaded, the local stress at the crack tip region will be high. The stress at the crack tip will be number of times higher than the applied nominal stress. This is called stress concentration. This stress concentration occurs due to interruption of load paths by the crack. This crack, upon cyclic stress, grows in size. The crack growth is slow process and depends upon stress field in the crack tip. The stages of crack growth due to fatigue is shown in Fig: 1.3. If the crack size exceeds certain length (critical crack length), sudden separation of material occurs which is called fracture. The LEFM method considers material to be elastic, following Hooke's law. EPFM method considers non-linear behavior of material. Although EPFM seems more realistic, LEFM can be used if the plastic zone is confined to small region around crack tip (Andersion, 2005). The size of crack tip depends upon toughness and yield strength of material. If toughness is less and/or yield strength is high, size of plastic zone is less (Broek, 1988) and LEFM is applicable. Hence for structural

steels, LEFM can be used. LEFM uses a parameter called stress intensity factor (K) to represent the stress field around the crack tip. Stress intensity factor depends upon applied nominal stress, crack size and geometric factor of the specimen. The most popular equation of crack growth, Paris equation is used for this research.

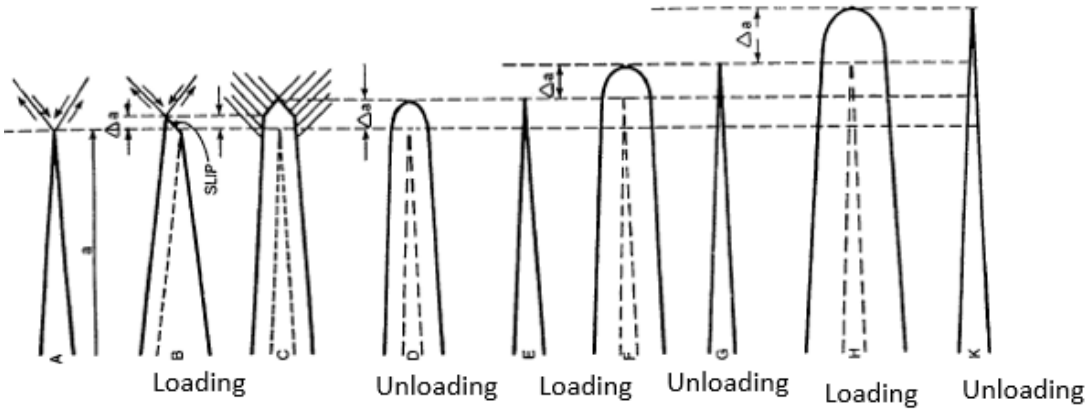

Fig: 1.3 Crack growth stages

In context of Nepal, there are many old bridges where the road surface above decking slab is deteriorated and new bridges where the road surface above the decking slab will deteriorate in time. This may affect the fatigue life of the bridge. Hence, this research intends to study the fatigue life of existing steel bridges due to different road surface condition.

1.3 Objective of Study

The objective of the study is **Fatigue life analysis of steel-concrete composite bridge considering road surface condition.** The general objectives of this study are listed below:

- To calculate fatigue life of steel-concrete composite bridge at flange-cover plate weld connection
- To compare fatigue life of steel-concrete composite bridge with different road surface conditions (Good, Average and Poor).
- To compare fatigue life of steel-concrete composite bridge with different vehicle velocities.

1.4 Methodology

This section describes the methodology followed to obtain the above-mentioned objectives which are as follows:

- Road Surface Profile Modeling
- Vehicle Modeling
- Arbitrary Bridge Modeling
- Solving Dynamic Equations of vehicle and Bridge to obtain stress time history in bridge due to vehicle and bridge interaction
- Cycle counting to convert variable amplitude stress history to number of constant amplitude sinusoidal stress histories by using Rain Flow Algorithm
- Damage model is used to find the overall effect of each converted constant amplitude of stresses on fatigue damage.
- Establish crack growth model and find the number of cycles failure for each road surface condition
- The process is repeated for different velocities of vehicle.

The methodology is described later in Chapter 3 in details. The brief methodology is shown in Fig: 1.4 as a flowchart.

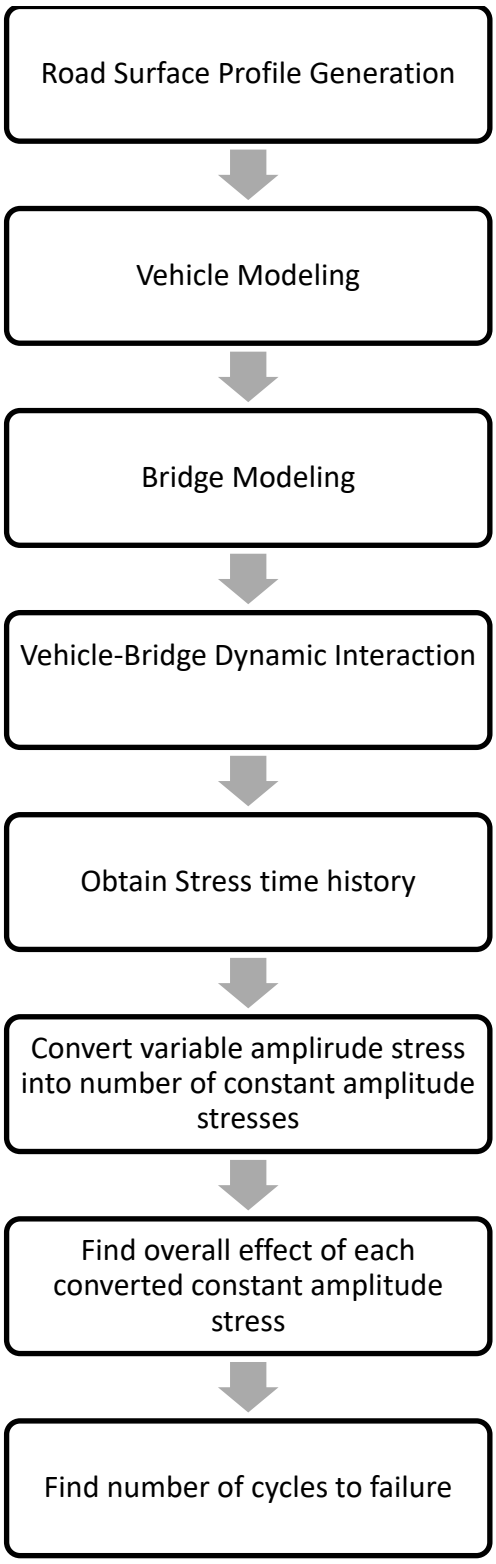

Fig: 1.4 Flow Chart representing methodology

CHAPTER 2: LITERATURE REVIEW

For this research, many kinds of literature related to vehicle bridge interaction problem, generation of road surface roughness, and analysis of fatigue performance of bridge are studied.

2.1 Road Surface Profile

Road surface profile can be artificially generated by considering road surfaces as homogeneous and isotropic two-dimensional Gaussian random processes (Dodds & Robson, 1973). This road surface profile generated by this method can be used for dynamic analysis of the vehicle and bridge system (Zhang & Cai, 2012; Yu, Wang, Li, Zhang, & Zhang, 2018; Deng, Wang, & Cai, 2016).

2.2 Vehicle Bridge Interaction

Vehicle bridge interaction (VBI) problem means solving differential equations of vehicle spring-mass system and bridge system. There are two primary methods for solving VBI problem: a) based on an uncoupled iterative procedure where equations of motion of bridge and vehicle are solved separately and b) those based on the solution of the coupled system, i.e., there is a unique matrix for the system that is formed by eliminating the interaction forces appearing in the equations of motion of bridge and vehicle, and updated at each point in time. Green, Cebon, & Cole,1995 solved both vehicle and bridge equations separately by using the iterative process. Similar kinds of the iterative process are studied by other researchers (Chatterjee, Datta, & Surana, 1994; Hwang & Nowak, 1992;Huang, Wang, & Shahawy, 1992). In these papers, the vehicle equation was solved first taking road surface profile as input. The results obtained by this solution are displacement of wheel and contact force. It is assumed that at the contact point between vehicle and bridge, the displacement is the same. The same contact force at wheel is applied to bridge to compute bridge displacement. Then the displacement is added to the road profile and again vehicle equation is solved. This process is repeated until the displacement obtained in (i)th and (i+1) th iteration is approximately the same. In the paper by Huang et al (2014) the vehicle and bridge both are modeled in ANSYS and iterative algorithm is developed to solve the interaction problem. In another research paper, the vehicle spring-mass system is solved by using SIMULINK, and the forces obtained from it are applied to bridge which is modeled in ANSYS (Yu, Wang et al, 2018). Similarly, various researchers Henchi, Fafard, Talbot, & Dhatt, 1998; Cai, Shia, Araujo, & Chen, 2007; Deng & Cai, 2010; Shi, Cai, & Chen,

2015 solved VBI problem by coupled method. In the coupled method, the bridge and vehicle equation motion are combined through the interaction force between them. Wang et al, 2014 ; Wang et al 2015 solved VBI problem by coupled method by using ANSYS. Both bridge and vehicles are modeled in ANSYS and coupled using ANSYS APDL.

For this research, iterative method is used as it is simpler and can be easily used using commercial finite element analysis software.

2.3 Fatigue Life Estimation

Fatigue analysis of bridge by LEFM approach is done in various research papers (Zhao, Haldar, & Breen, 1992), (Zhao, Haldar, & Jr, 1994), (Zhao & Haldar, 1996), (Pugno et al, 2006). Although these research papers consider crack growth for fatigue analysis, the effect of road surface profile on crack propagation that affects fatigue life of the bridge is not considered. Zhang & Cai(2012); Deng, Wang, & Cai (2016) considered road surface roughness and solved vehicle bridge interaction problem to study fatigue performance of the bridge. However, in both of the papers, the AASHTO method is used which cannot incorporate crack growth mechanism.

The S-N curve provided by AASHTO only gives relationship between the stress range(S) and the remaining life(N) of the bridge. This method provided by AASHTO can be used for designing new bridge. For the inspection of old bridge, crack size information is important and AASHTO doesn't provide it. If the size crack in the material is more, the fatigue life of material is less because the crack propagation rate depends upon stress intensity factor (Paris, 1961) which inturn depends upon crack size. More is the crack size, more is the stress intensity factor and hence more is the crack growth rate. The also stress intensity factor depends upon geometry of the specimen. Tada & Irwin(1975) ; Zettlemoyer (1976); Zettlemoyer & Fisher (1977); Zettlemoyer & Fiisher (1978); Yazdani & Albrecht(1990) have used different correction factors for different geometries. The Paris equation is based on constant amplitude loading but for most of the practical cases, including, the stress amplitude is random and varying. To solve problem for variable amplitude loading, there are different approaches. First of all, the variable amplitude load cycle is to be converted to number of constant amplitude load cycles. It includes countng number of cycles of each constant amplitude loads. This count is to be done by cycle counting method. There are number of cycle counting methods. They are rain flow counting method (Endo, Mitsunaga, Takahashi, Kobayashi, & Matsuishi, 1974) , Peak Method

(ASTM Standard E1049, 2001), range method (ASTM Standard E1049, 2001), Range-pair Method (ASTM Standard E1049, 2001) etc. After the number of cycles for each amplitudes are found out, damage accumulation model must be used. This model combines the effect of every constant amplitude loadings in fatigue crack propagation. The damage models are of two types. One is linear damage model and another is non linear damage model. Linear damage model assumes that damage produced by variable amplitude loading is linear sum of various constant ampitude loading. It assumes that all cycles of load promote in crack propagation and cycles of different sizes do not interact to accelerate and retard the growth (R.Narayanan & T.M.Roberts, 2005). The best known linear damage model is given by Miner, 1945. Another method of modeling damage acumulation is non- linear damage accumulatuon method. It assumes that all cycle of load do not promote for crack growth. Damage produced by one cycle is affected by damage produced by another cycle. According to Broek, 1988, if there is stress overload, the crack growth rate decreses due to development of residual compressive stress in the plastic zone after unloading. For stress variations whose stress ratio (R), which is the ratio of mimimum stress to maximum stress is high, we can use linear damage models (Andersion, 2005). For bridges, as there is already presence of dead load, the stress ratio is high, hence use of linear damage model is justified.

2.4 Literature review conclusions

From these literature reviews, it is clear that further research on the effect of road surface profile on fatigue life of steel bridge by incorporating crack growth mechanism is required.

CHAPTER 3: THEORITICAL BACKGROUND AND METHODOLOGY

3.1 Artificial Road Surface Profile Generation

To capture the dynamic interaction between vehicle and bridge, first of all, we need the road surface profile data. The road profile is the variation of height of road along the length. The road surface profile may be measured in-situ by the help of instruments like profilometers etc. But these instruments require considerable costs and time for precise measurement of the road surface profile. Hence, in this study, road surface profiles are artificially generated by the help of ISO8608 standards.

ISO 8608 standard models road profile by using fundamental concepts of spatial frequency and Power Spectral Density (PSD). The spatial frequency is the frequency of road profile varying along spatial length. It is defined in cycles per meter. IS8608 is based on assumption that the road surface is combination of large number of shorter and longer periodic bumps with different amplitudes. It includes calculation of PSD of vertical displacements $\varphi(n)$ as a function of spatial frequency 'n'.

The road surface is classified on the basis of $\varphi(n_o)$, which is the PSD calculated corresponding to conventional value of spatial frequency n_o=0.1 cycles/m. The values of $\varphi(n_o)$ proposed by ISO8608 according to the different road classes (A to H) are tabulated in Table 1.

Table 1 Values of $\varphi(n_o)$ proposed by ISO8608

Road Class		
Upper Limit	Lower Limit	φ (n_o) (10^{-06} m^3)
A	B	32
B	C	128
C	D	512
D	E	2048
E	F	8192
F	G	32768
G	H	131072

So, PSD for other spatial frequencies is given by,

$$\varphi(n) = \varphi(n_o)\left(\frac{n}{n_o}\right)^{-2} \tag{3.1}$$

If 'L' is the length of the road profile and 'B' be the sampling interval, the maximum theoretical sampling frequency is given by,

$$n_{max} = \frac{1}{B} \tag{3.2}$$

Hence, the length L is divided into N_L segments given by,

$$N_L = \frac{L}{B} \tag{3.3}$$

Also, the minimum spatial frequency is given by,

$$\Delta n = \frac{1}{L} \tag{3.4}$$

Other spatial frequencies (called generic spatial frequencies) can be written as,

$$n_k = k * \Delta n \tag{3.5}$$

Where, k = 1 to N_L

Hence, the road surface profile is generated through inverse Fourier Transformation as (Wang & Huang, 1992):

$$r(x) = \sum_{k=1}^{N_L} \sqrt{2\varphi(n_k)\Delta n}\cos\left(2\pi(n_k)x + \theta_k\right) \tag{3.6}$$

Where, "Θ_k" is random phase angle with uniformly distributed from 0 to 2π, "$\varphi(n_k)$" is the power spectral density (PSD) function (m^3/cycle/m) and "n_k" is the k^{th} spatial frequency (cycle/m).

The PSD values corresponding to conventional value of spatial frequency $\varphi(n_o)$ for various road surface condition are given by ISO 8608 standard. ISO 8608 classifies eight classes (A to H) of road surface roughness. The road condition which is more degraded than poor condition i.e., very poor road condition is not considered in this study. The very poor road condition caused vehicle to bounce and caused tire to lose contact from road. Hence, for this study, only three classes of road surface, A-B (Good), B-C (Average) and C-D (Poor) are taken.

3.2 Vehicle Modeling

The vehicle chosen for fatigue analysis is standard HS20-44, a tractor and trailer model truck proposed by AASHTO. To capture dynamic behavior of the vehicle, it is modeled as three dimensional multi degree of freedom (MDOF) system. The vehicle is modeled according to Zhang & Cai (2012), which is standard HS20-44 truck and is shown in Fig: 3.1. The vehicle bodies are modeled as rigid bodies having mass and moment of inertia each with three degrees of freedoms (vertical displacement, pitching and rolling rotations). As the HS20-44 is tractor-trailer modeled, both the tractor and trailer are modeled as rigid bodies. Each tire is modeled as lumped mass with one degree of freedom (vertical displacement). The tire and suspension are considered as springs with their respective stiffness and damping coefficients. There exists compatibility condition at the connection between tractor and trailer, which is, the vertical displacement at the connection is same for both tractor and trailer. Altogether, the whole MDOF system consists of 11 independent degrees of freedoms. The Vehicle parameters are shown in Table 2. The vehicle parameters include mass, moment of inertia (pitching and rolling), lengths, stiffness and damping coefficients. In this way the MDOF system of vehicle is established.

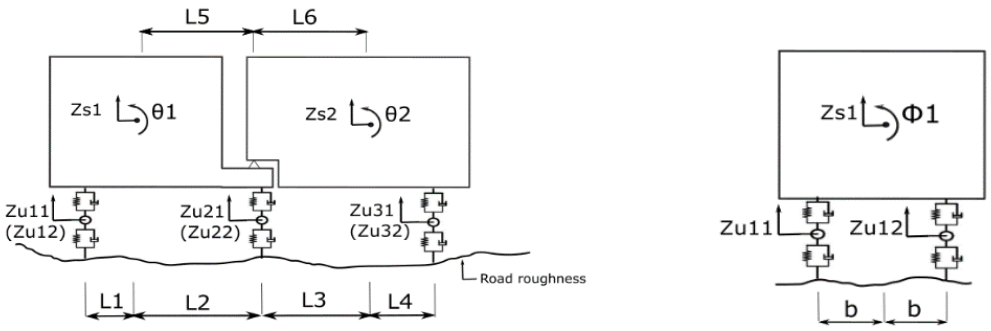

Fig: 3.1 Vehicle Model Front view and Side View

Now, to solve the MDOF system, equation of motion of the system must be established. The equation of motion of the system is established from Lagrange's equation which is given by

$$\frac{\partial}{\partial t}\left(\frac{\partial L}{\partial \dot{q}_i}\right) - \left(\frac{\partial L}{\partial q_i}\right) = 0 \tag{3.7}$$

Where, L= T-V; which is the Lagrangian

T= Kinetic Energy of the system

V= Potential Energy of the system

q_i=Generalized coordinate according to degrees of freedom.

Table 2 Vehicle Parameters

Mass	Body of Truck 1 Body of Truck 2 Suspension of 1st Axle Suspension of 2nd Axle Suspension of 3rd Axle	12612 kg 26113 kg 490 kg 808 kg 653 kg
Moment of inertia	Pitching, body 1 Pitching, body 2 Rolling, body 1 Rolling, body 2	2022 kgm^2 33153 kgm^2 8544 kgm^2 181216kgm^2
Spring stiffness	1st Upper axle 1st axle Lower axle 2nd Upper axle 2nd Lower axle 3rd Upper axle 3rd Lower Axle	242604 N/m 875082 N/m 1903172 N/m 3507429 N/m 1969034 N/m 3507429 N/m
Damping Coeffieient	1st Upper axle 1st axle Lower axle 2nd Upper axle 2nd Lower axle 3rd Upper axle 3rd Lower Axle	2190 Ns/m 2000 Ns/m 7882 Ns/m 2000 Ns/m 7182 Ns/m 2000 Ns/m
Length	L1 L2 L3 L4 L5 L6 B	1.698 m 2.569 m 1.984 m 2.283 m 2.215 m 2.338 m 1.1 m

As the MDOF consists of 11 independent degrees of freedom, 11 independent equations of motion can be established. The equation of motions can be derived for each generalized coordinates and can be solved using commercially available software like MATLAB SIMULINK. But, for the three-dimensional MDOF system like this vehicle, the manual derivation and solution of the equation of motion is tedious job. Hence, for this study, Finite Element Modeling (FEM) of the MDOF system is done. The FEM modeling is done in ANSYS-APDL software.

In ANSYS, various types of elements have to be assigned for various MDOF components. The lumped mass are modeled as MASS21 element, the springs and dampers are modeled as COMBIN14 element and the vehicle body is represented as MPC-184 elements. The brief explanation of these elements is discussed below:

- MASS21 element

  It is the point element with single node. The node has six degrees of freedom. Three degrees of freedom are translation in nodal X, Y and Z direction while other three degrees of freedom are rotation about nodal X, Y and Z axes. The data to be input for this element are mass and moment of inertia in each coordinate direction. Various options for mass element are available like, 3D mass with rotary inertia, 3D mass without rotary inertia, 2D mass with rotary inertia and 2D mass without rotary inertia. For the MDOF system modeling of the vehicle in this study, vehicle body mass is modeled as 3D mass with rotary inertia and tire mass is modeled as 2D mass without rotary inertia.

- COMBIN14 element

  It is two-noded spring-damper element. There are two types of spring-damper elements available. They are, longitudinal spring damper and torsional spring-damper. The longitudinal spring damper is uniaxial compression-tension element with three degrees of freedoms (translations in X, Y and Z directions) in each node. The torsional spring-damper element is the rotational element with three degrees of freedom (rotation about X, Y and Z axes) at each node. The data to be input for this element are spring stiffness coefficient and damping coefficient. The longitudinal spring elements are used for modeling springs of vehicle suspension and tires.

- MPC184 element

It is two-noded element which acts as rigid constraint between two deformable bodies. It acts as rigid body that transmits forces and moments. There are two types of MPC184 element. First type is rigid link element which has three degrees of freedom (translation in X, Y and Z directions) and the second type is rigid beam (translations in X, Y and Z directions with rotation about X, Y and Z axes). As it is rigid element, material and stiffness data need not to be provided as input. The vehicle body for tractor and trailer is modeled by rigid beam element. Also, the compatibility condition at the connection between the tractor and trailer is also established.

The FEM modeling of the vehicle is done in ANSYS-APDL software by using elements mentioned above and is shown in Fig: 3.2

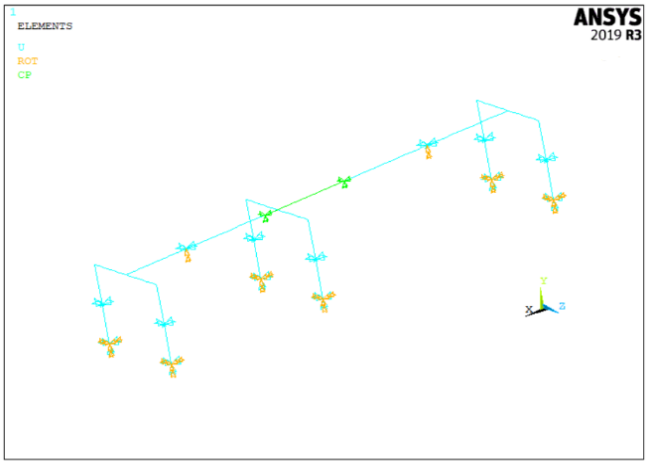

Fig: 3.2 FEM model of Vehicle in ANSYS APDL

3.3 Bridge Model

The objective of this study is to carry out fatigue analysis of steel-concrete composite bridge. The fatigue crack growth is analyzed at the welded cover plate at the tension flange of the girder. To find the stresses required for fatigue analysis, the bridge is to be modeled and loads must be applied. A typical bridge is taken for this study and its parameters are tabulated in Table 3.

Table 3 Bridge Parameters

Parameters	Value
Span Length	25 m
Number of Girders	4
Spacing of Girders	3 m
Number of lanes	2
Web depth	1300 mm
Web Thickness	10 mm
Flange Width	400 mm
Flange Thickness	31.37 mm
Cover Plate Thickness	25 mm

The finite element modeling is done in ANSYS -APDL software. Different element types can be used for different bridge components. Various literatures suggested the following approaches:

- Using solid element (Brick element) for deck and girder
- Using solid element for deck and Shell elements for girder (flanges + web)
- Using Shell elements for both deck and girder (flanges + web)
- Using shell elements for deck & web and beam element for flanges

The solid model requires a large number of nodes and computation time. According to Chung & Sotelino(2005), the shell element is suitable for modeling a bridge deck than by using the solid elements. For this research purpose, both deck and girder are modeled as a shell element.

As mentioned earlier, flange, web, and deck are modeled by using shell elements. By default, the nodes lie in the mid surface of the shell element. In real life, the connection between flange and web is not at the mid surface of the flange. So, offset is provided so that the model gives a realistic result. Also, the top flange and deck are connected by Multi-Point Constraint (MPC184) element, which is the rigid link. It also makes sure that the top face and bottom face of the deck are connected. Chung & Sotelino(2005) did the same modeling of girder and deck using shell modeling as shown in Fig: 3.3

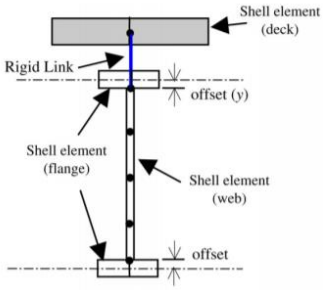

Fig: 3.3 Girder model by Chung & Sotelino (2005)

. So, for this study,offset and rigid links are provided such that it models a realistic connection between the top face of the flange and the bottom face of the deck. The model is shown in

Fig: 3.4

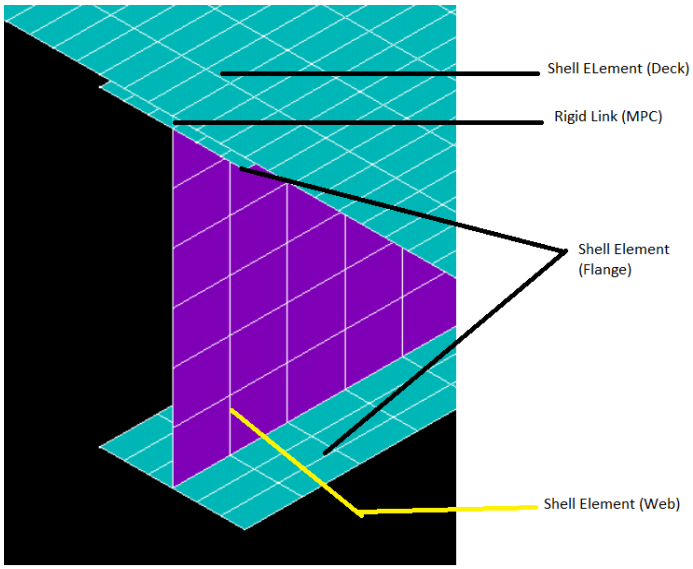

Fig: 3.4 FEM model of girder showing flange, web and their connection with rigid link

ANSYS provides shell element as SHELL181 element. It is four noded area element. Each node has six degrees of freedom (three translations in X, Y and Z direction and three rotations about X, Y and Z axes). This element supports both reduced integration and full integration scheme. The reduced integration scheme uses fewer points (gauss points) to integrate (to calculate stiffness matrix) while the full integration scheme uses all points to integrate. The reduced integration scheme includes less calculation and the computation time is faster than that of full integration scheme. But there is one disadvantage of using reduced integration scheme. As there are smaller number of integration points in reduced integration scheme, there may be such condition (usually in in-plane bending condition)

where the strains at those points are zero resulting in zero strain energy state. This causes jogging of mesh during the deformation. This effect is called hour glass effect. Due to hour glass effect, the structure modeled doesn't represent the actual structure and hence there exist error in modeling.

For this study, initially both reduced and full integration scheme models are used. No hour glass effect is seen in reduced integration scheme model and the results form the both models are obtained similar. Hence, for this study, the shell elements in the bridge model are modeled according to reduced integration scheme. Similarly transverse stiffeners and cover plates are modeled by SHELL181 element. The cross bracings are modeled as BEAM188 element, which is the 3D frame element.

It is assumed that the support condition for the bridge is simply supported. Hence, the boundary condition the bridge modeled is provided accordingly. The lowermost part of one end is restrained at all three directions and the lowermost part of another end is restrained in vertical and transverse direction i.e., free at the longitudinal direction.

The overall Finite Element Model of bridge is shown in Fig: 3.5

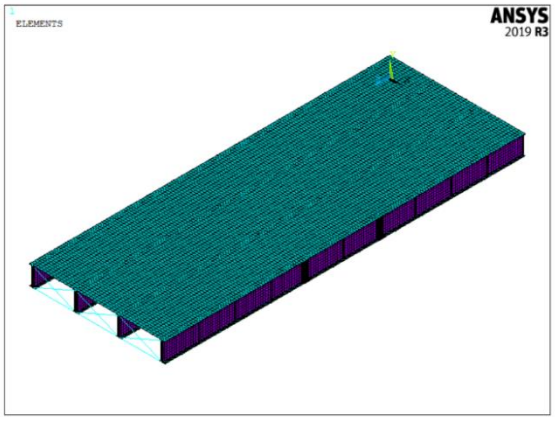

Fig: 3.5 FEM model of Bridge in ANSYS APDL

3.3.1 Bridge Damping Modeling

Rayleigh damping model is used to model damping of the bridge. The damping matrix of the bridge is assumed to be proportional to combination of mass and stiffness matrices as,

$$[c_d] = \alpha[m] + \beta[k] \tag{3.8}$$

Where,

$[c_d]$ is damping matrix of bridge structural system

$[m]$ is mass matrix of bridge structural system

$[k]$ is stiffness matrix of bridge structural system

α and β are mass proportional and stiffness proportional constants.

The damping ratio for mass proportional damping is given by,

$$\xi_n = \frac{\alpha}{2\omega_n} \tag{3.9}$$

And the damping ratio for stiffness proportional damping is given by,

$$\xi_n = \frac{\beta\omega_n}{2} \tag{3.10}$$

Where, ω_n is the n^{th} natural frequency of bridge structural system.

The Rayleigh damping combines both mass and stiffness proportional damping. The relationship between damping ratio and natural frequency is hence given by,

$$\xi_n = \frac{\alpha}{2\omega_n} + \frac{\beta\omega_n}{2} \tag{3.11}$$

Now, the evaluation the values of α and β can be done by forming a pair of simultaneous equations if the values of damping ratios ξ_m and ξ_n associated with two specific natural frequencies ω_m, ω_n are known. The relationship between the damping ratio and natural frequency for Rayleigh damping is shown in Fig: 3.6.

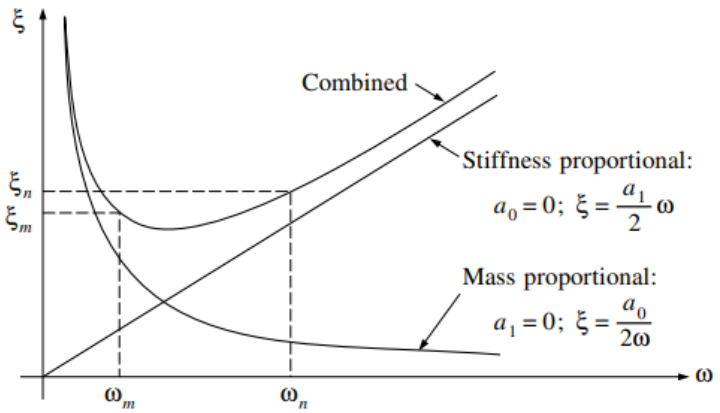

Fig: 3.6 ξ vs ω relationship for Rayleigh Damping

It is assumed that both damping ratios associated with control frequencies ω_m and ω_n are equal i.e., $\xi_m = \xi_n = \xi$. Hence, the pair of simultaneous equation gives the solution as,

$$\begin{bmatrix}\alpha\\ \beta\end{bmatrix} = \frac{2\xi}{\omega_m + \omega_n}\begin{bmatrix}\omega_m\omega_n\\ 1\end{bmatrix} \tag{3.12}$$

In this way, the coefficients α and β can be calculated. The control frequency ω_m is taken as first fundamental natural frequency while ω_n is the highest frequency that contributes in dynamic response of the bridge. The damping ratio ξ associated with the control frequencies ω_m and ω_n is taken as 0.03 (Leitão et al, 2013).

3.4 Vehicle Bridge Interaction Modeling

Solving the equation of motions of both bridge and vehicle is called the vehicle bridge interaction problem. The vehicle is considered as a spring-mass system. The bridge system consists of girders and slabs with their respective mass and stiffness.

The iterative method is adopted for solving the VBI problem as this method is easy to apply on commercially available finite element modeling software. Equation of motions of vehicle and bridge are solved separately. The vehicle and the bridge are connected by tire contact force equal to the weight of the vehicle plus force in tire springs.

Steps for the iterative method for solving the VBI problem are as follows:

a. First of all, the bridge is considered as a rigid structure. The equation of motion of the vehicle is solved considering road surface undulation profile as input force (k*r(x,t) and c_{vd}*ṙ(x,t)). The displacement $u_v(x,t)$ and velocity $\dot{u}_v(x,t)$ of vehicle masses are obtained. Where, k is stiffness and c_{vd} is damping coefficient of vehicle.
b. The tire contact forces (function of space and time) are calculated; which is sum of weight of vehicle and tire spring forces: k*{ $u_v(x,t)$ - r(x,t) } + c_{vd} *{ $\dot{u}_v(x,t)$ - ṙ(x,t) }
c. This contact forces which is the function of space and time is applied to bridge to obtain displacement $u_b(x,t)$ and velocity $\dot{u}_b(x,t)$ of the bridge

d. The road surface undulation profile is updated by adding bridge displacement to obtain updated road input force in vehicle as:

$$k*r(x,t) + k*u_b(x,t) \text{ and}$$

$$c_{vd} *\dot{r}(x,t) + c_{vd} * \dot{u}_b(x,t)$$

e. The updated road input force is then applied to the vehicle to obtain new displacement $u_v(x,t)$ and velocity $\dot{u}_v(x,t)$ of vehicle masses.

f. The tire forces are calculated as $k* \{ u_v(x,t) - r(x,t) - u_b(x,t) \}$ and $c_{vd} *\{ \dot{u}_v(x,t) - \dot{r}(x,t) - \dot{u}_b(x,t) \}$. This force is summed with weight of vehicle and applied to bridge to obtain new displacement $u_b(x,t)$ and velocity $\dot{u}_b(x,t)$.

g. Step 'd' to 'f' is repeated until convergence in value of displacements in i^{th} and $i^{th}+1$ iteration occurs.

This iteration can be done by in FEM software, ANSYS Parametric Design Language (APDL).

3.5 Rain Flow Cycle Counting

The result obtained from Vehicle Bridge Interaction is stress vs time plot. The stress vs. time plot is not sinusoidal with constant amplitude but is of variable amplitude. As we know number of reversals of stress gives damaging effect of fatigue, we need to isolate number of cycles for each stress amplitude. This is done with the help of Rain Flow cycle counting algorithm (Endo et al, 1974). This algorithm separates the variable amplitude stress time history into number of constant amplitude stresses with corresponding number of cycles. The result of Rain Flow cycle counting algorithm can be directly used in fatigue analysis as Rain Flow cycle counnting algorithm is on the based on hysteric behaviour of material. One hysteresis loop results in one full cycle. This algorithm models material memory effect seen with stress-strain hysteric cycle.

A MATLAB program is written on the basis of this algorithm an number of cycles for given stress time history is obtained. Form this, we can obtain stress range ($\Delta\sigma_i$) and its corresponding number of cycles (N_i).

3.6 Fatigue Crack Growth Model

To estimate fatigue life using LEFM, crack growth model based on Paris Law (Paris, 1961) is used which is given by:

$$\frac{da}{dN} = C(\Delta K)^m \tag{3.13}$$

Where, $\frac{da}{dN}$ is crack growth rate; *ΔK* is stress intensity factor range; *C* and *m* are material constants. For mild steel, value of m is taken as 3.0. The value of crack growth constant, is taken as 2.05×10-10ksi√in which is the average value of crack growth constant (Hirt & Fisher, 1973). This value of constant *C*, which is the average value of crack growth constant is also used by Zhao et. al. (1994) for mild steels.

The value of stress intensity not only depends upon applied stresses but also depends upon crack shape, weld size and geometric detail of bridge. Paris gave the crack growth rate formula for infinite plate with central through crack. So, to account the effect of crack shape, weld size and geometric detail of the bridge, the correction factors are used. The correction factors are namely, shape correction factor (Fe), finite width correction factor (Fw), free surface correction factor (Fg) and stress gradient correction factor (Fs). For this study, crack growth at weld toe of cover plate is analyzed. The correction factors for welded cover plate are as follows (Fisher, 1984):

- Shape Correction Factor (Fe)

  It takes into account for shape of the crack front. The crack is assumed as semi-elliptical in shape. The shape correction factor (Fe) is given by (Fisher, 1984):

$$F_e = \frac{1}{\int_0^{\frac{\pi}{2}} \sqrt{1 - \frac{c(a)^2 - a^2}{c(a)^2} \sin^2(\Theta)\, d\theta}} \tag{3.14}$$

Where, 'a' is the crack depth, 'c' is half crack length which is the function of crack depth, and 'θ' is the angle for an elliptical crack. Half crack length and crack depth are related as (Fisher, 1984): $c(a) = 5.457\ a^{1.133}$; units in inches.

- Finite width Correction factor (Fw)

It takes into account for the width of specimen (in this case bottom flange of girder). The finite width correction factor (Fw) is given by:

$$F_w = \left(\sec\left(\frac{\pi a}{2b}\right)\right)^{\frac{1}{2}} \tag{3.15}$$

Where, 'a' is the crack depth and 'b' is half flange width of girder.

- Free Surface Correction Factor (Fs)

The crack growth rate equation developed by Paris is for through crack. But in the case of fatigue crack in flange of bridge, the crack originates at the surface of the flange and grows inside it. This type of crack is called surface crack and is corrected by free surface correction factor (Fs) and is given by (Fisher, 1984):

$$F_s = 1.211 - 0.186\sqrt{\frac{a}{c(a)}} \tag{3.16}$$

Where, 'a' is the crack depth and 'c' is half crack length

- Stress Gradient Correction Factor (Fg)

At the flange and cover plate connection, there will be stress concentration i.e the stress will be high in the vicinity of the connection. As from the VBI analysis, we take nominal value of stress, the stress must be corrected for the stress gradient. Hence, the Stress Gradient Factor is given by (Fisher, 1984):

$$F_g = \frac{-3.539 \ln\left(\frac{Z}{t_f}\right) + 1.981 \ln\left(\frac{t_{cp}}{t_f}\right) + 5.798}{1 + 6.789\left(\frac{a}{t_f}\right)^{0.4348}} \tag{3.17}$$

Where, 'a' is the crack depth, 'Z' is weld leg size, 't_f' is thickness of flange, 't_{cp}' is thickness of cover plate

The stress intensity range in terms of stress range and crack size with correction factors is finally obtained as:

$$\Delta K = F_g F_w F_s F_e \overline{\Delta\sigma} \sqrt{\pi a} \tag{3.18}$$

Where, $\overline{\Delta\sigma}$ is the equivalent stress range, obtained from rain flow cycle counting and linear damage rule.

Finally, rearranging Paris law equation, we get

$$N = \int_{a_i}^{a_f} \frac{da}{C(\Delta K)^m} \tag{3.19}$$

Where, N is number of cycles to failure, a_i and a_f are initial and final crack size. These cracks are the cracks in the flanges in flange-cover plate weld connection. According to Albrecht & Yazdani (1986), initial crack size 'a_i' is log normally distributed and mean

value is taken as 0.51mm (0.02 in). According to Barsom & Rolfe (1987), crack size of 10.2mm (0.4 in) in cover plate will fail by fatigue regardless of level of fracture toughness of steel. Hence, this value, 10.2 mm is taken as final crack size *'a_f'.*

3.7 Linear Damage Rule

After obtaining stress range corresponding to number of cycles, we need to find out total damage due to each stress ranges. It can be done by linear or non-linear damage rule. The linear damage rule assumes that all the stress ranges take part in fatigue crack growth. According to linear damage rule, the equivalent stress range ($\overline{\Delta\sigma}$) is obtained by (Fisher, 1984):

$$\overline{\Delta\sigma} = \left(\sum_{i=1}^{n} \frac{\Delta {\sigma_i}^m N_i}{N_{tot}} \right)^{\frac{1}{m}} \tag{3.20}$$

Where, '$\Delta\sigma_i$' is ith stress range, 'N_i' is the corresponding number of cycles and 'N_{tot}' is the total number of cycles.

Experimentally it has been found that, due to sudden stress overload, the crack growth rate is retarded. This retardation is caused due to residual compressive stress just after the stress overload. This results in closure of crack and hence reduces the crack growth rate. To account the effect of crack closure phenomenon, the non-linear damage rule is used.

The linear damage rule is simple and easy to use while non-linear damage rule is cumbersome to solve. In some practical cases however, crack closure phenomenon can be neglected. Such case normally occurs when cyclic loading involving high stress ratio (ratio of minimum stress to maximum stress), where crack closure phenomenon is negligible. The structures like steel bridges, whose dead load is high, stress ratio is high (ratio of minimum stress to maximum stress). So, crack closure effect can be neglected for fatigue analysis in bridge. Hence, for this study, linear damage rule is used.

CHAPTER 4: RESULTS AND DISCUSSIONS

4.1 Road Surface Roughness Generation

Three road classes, A-B (Good), B-C (Average) and C-D (Poor) are generated using (3.6 in MATLAB (MathWorks). The sample of the generated surface profiles are shown in Fig: 4.1.

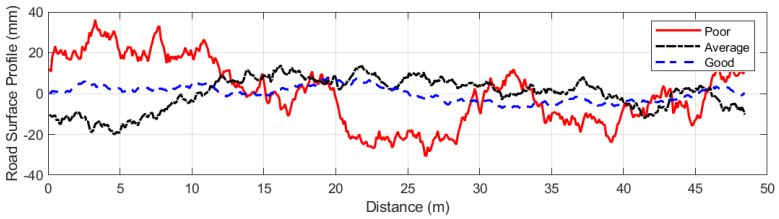

Fig: 4.1 Road Surface Profile for Good, Average and Poor Condition

4.2 Bridge modal and Damping Analysis

As the damping is considered according to Rayleigh damping (Leitão et al, 2013), modal analysis of bridge is done to obtained natural frequencies of bridge, from which mass (α) and stiffness (β) proportionality constants are determined. The natural frequencies of bridge are shown in Table 4. To demonstrate the natural frequencies, the first to seventh mode shape of the bridge are shown in Fig: 4.2 to Fig: 4.8. From the modal analysis it is seen that, the modes of vibrations of bridge from mode 1 to 7 have displacements of girder and deck slab in vertical and horizontal directions. The higher modes (beyond mode 7) have mode shapes that have displacement of crossties only, which is not significant mode of vibration for vehicle loading. Hence, to find α and β, first mode and seventh mode frequencies are taken as lower and upper bound frequencies (control frequencies). The damping ratio is taken as 0.03 (Leitão et al, 2013). The values of α and β are obtained as 1.36155 and 0.00042 respectively. These values are used for dynamic analysis of bridge.

Table 4 Natural Frequencies according to modes of vibration of bridge

Mode	Natural Frequency
	(Hz)
1	4.5173
2	5.72632
3	7.20553
4	13.6431
5	14.4608
6	14.915
7	18.0137

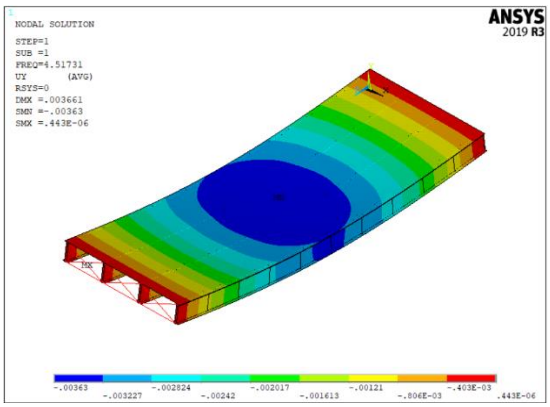

Fig: 4.2 Mode 1, 4.5173 Hz

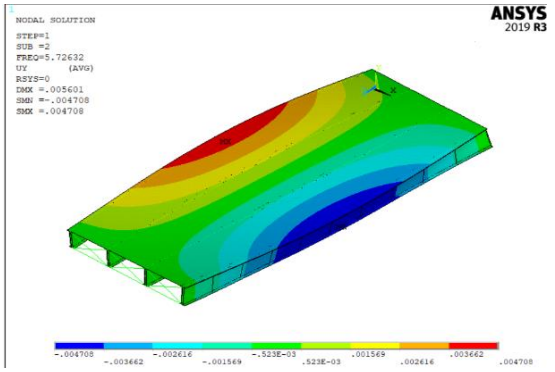

Fig: 4.3 Mode 2, 5.72632 Hz

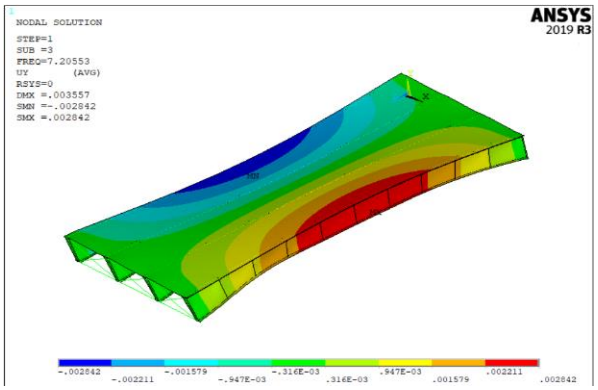

Fig: 4.4 Mode 3, 7.20553 Hz

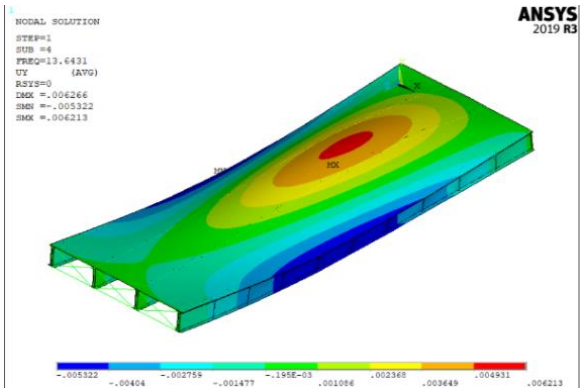

Fig: 4.5 Mode 4, 13.6431 Hz

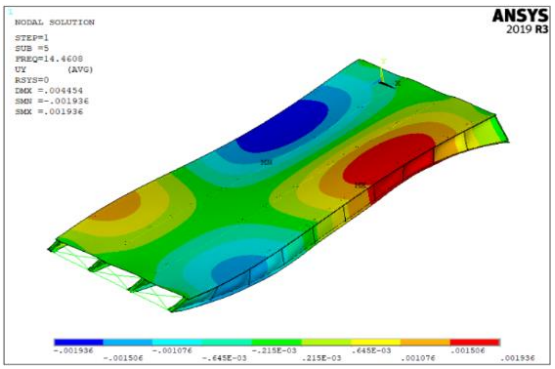

Fig: 4.6 Mode 5, 14.4608 Hz

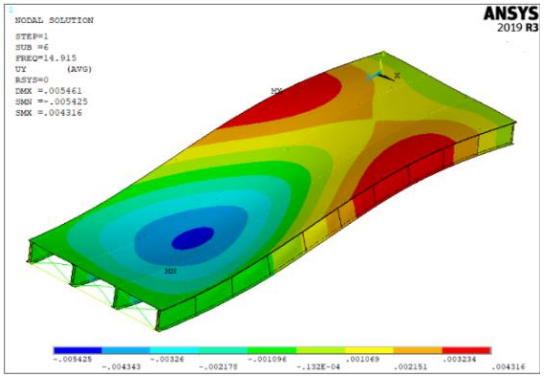

Fig: 4.7 Mode 6, 14.915 Hz

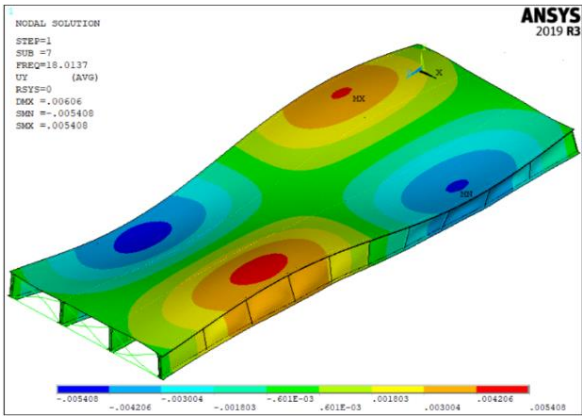

Fig: 4.8 Mode 7, 18.0137 Hz

The graph between damping ratio (ξ) and natural frequency (ω) for Rayleigh damping is shown in Fig: 4.9.

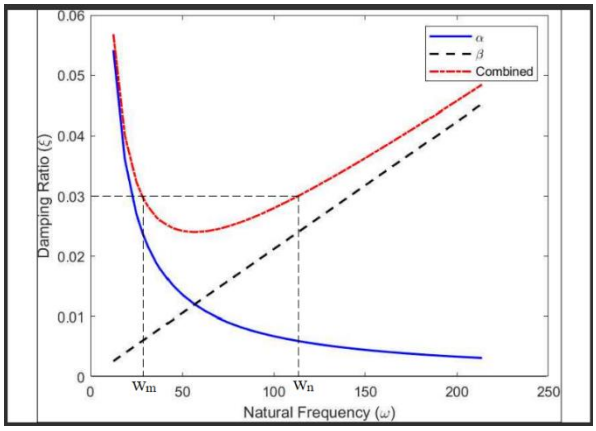

Fig: 4.9 ξ vs ω relationship for Rayleigh Damping, where, ω_m and ω_n are control frequencies

4.3 Validation

4.3.1 Vehicle Model Validation

The modal analysis of vehicle is done to extract its natural frequencies. As there are eleven independent degrees of freedom, eleven number of modes are extracted using ANSYS APDL. The natural frequencies obtained are compared with the natural frequencies obtained by Yang et al (2015). It is found that the natural frequencies obtained are exactly equal to that of the literature. It is tabulated in Table 5. Hence, the vechile model is verified.

Table 5: Comparisons of Natural Frequencies of Vehicle model for Validation

Natural Frequencies (Hz)		
Mode	Obtained in ANSYS	Obtained by Yang et al (2015).
1	1.52	1.52
2	2.14	2.14
3	2.69	2.69
4	5.94	5.94
5	7.74	7.74
6	7.82	7.82
7	8.92	8.92
8	13.87	13.87
9	13.99	13.99
10	14.63	14.63
11	17.95	17.95

4.3.2 Bridge Finite Element Model Validation

As the bridge model chosen is arbitrary, exact model of the bridge cannot be found in the existing literatures. So, the modeling algorithm used in ANSYS APDL is validated by modeling the 3-girder bridge from Jayakrishnan et al (2017). The natural frequencies obtained in ANSYS and obtained by the literature are tabulated in Table 6.

Table 6 : Comparisons of Natural Frequencies of Bridge model for Validation

Bridge Natural Frequencies (Hz)		
Mode	Obtained in ANSYS	Obtained by Jayakrishnan. et al (2017).
1	4.54	4.60
2	6.49	6.66
3	8.61	8.74
4	14.36	14.77
5	15.04	15.23
6	15.43	15.59

Hence, from Table 6 it is seen that the natural frequency calculated in ANSYS is somehow equal to that of obtained by Jayakrishnan. T, J & Lekshmi Priya; (2017).

4.4 Vehicle Bridge Interaction Analysis

To perform the vehicle bridge interaction, a code based on VBI iterative algorithm is written in ANSYS APDL. To verify the code, a two-mass spring system traversing on a simple beam is analyzed. The displacement time history obtained by Hawk & Ghali (1981) is compared with that of code and is shown in Fig: 4.10.

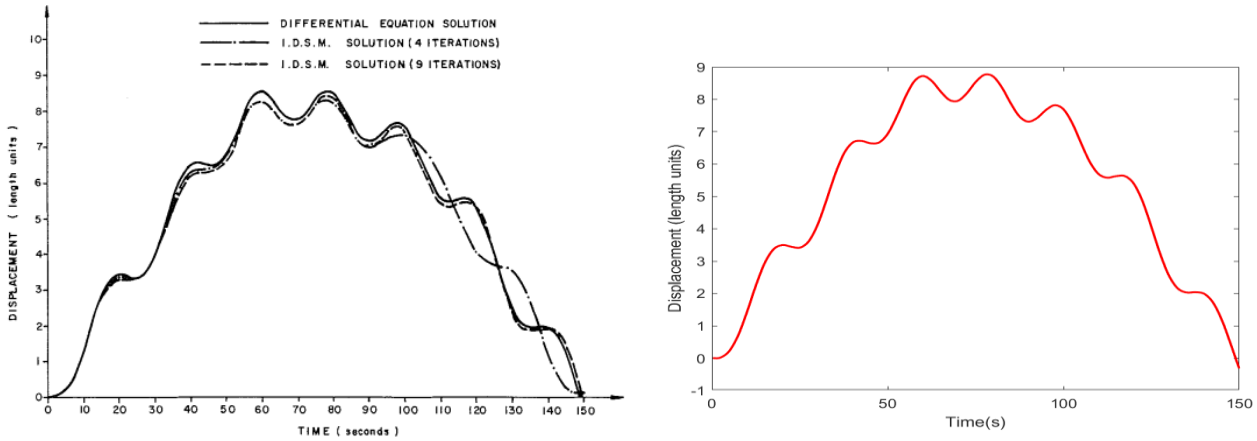

a) b)

Fig: 4.10 a) Displacement time history of simple beam obtained by Hawk & Ghali (1981) b) Displacement time history obtained from code

Vehicle bridge interaction is done using iterative method. Both vehicle and bridge are modeled in ANSYS APDL and solved. The displacement at midpoint of girder is checked after each iteration which converged at 7 iterations. The displacements at midpoint of girder after each iteration for poor road condition with vehicle velocity of 40 Kmph are listed in

Table 7. The VBI is done for three different road surface conditions by considering vehicle velocities of 20 Kmph, 40 Kmph, 60 Kmph, 80 Kmph and 100 Kmph. Hence, total 15 VBI analyses are done.

Table 7 Convergence of midpoint Displacement values at each iterations for poor road condition with vehicle velocity 40 Kmph

Iterations	Displacement at midpoint of girder (m)	Error % =
1	-7.95417E-03	
2	-1.00459E-02	26.30%
3	-1.04932E-02	4.45%
4	-1.05641E-02	0.68%
5	-1.05758E-02	0.11%
6	-1.05779E-02	0.02%
7	-1.05782E-02	0.00%

4.5 Fatigue Analysis

The stress time histories at the weld toe of the cover plate from every 15 VBI analyses are obtained. It is to be noted that stress range in Paris law equation (Eq. (3.13) is nominal stress range. According to Zettlemoyer (1976) nominal stress is obtained at the distance of roughly 2.5 times flange thickness from the weld detail. For this study, as the flange thickness of the girder is 31.37 mm, stress at the node 100 mm from the weld detail is taken. The stress time history of vehicle moving at different velocities on good, average and poor road surface condition is shown in Fig: 4.11 to Fig: 4.15.

Using rain flow cycle counting algorithm (Endo et al; 1974), the stress range and its corresponding number of cycles are obtained. The equivalent constant amplitude stress range is obtained by using (3.20).

The equivalent stress range obtained are tabulated in Table 8.

Table 8 Stress Range obtained for various velocity and road surface condition

Velocity (kmph)	Stress Range (MPa)		
	Good	Average	Poor
20	11.24	13.22	16.13
40	11.74	14.402	16.625
60	11.79	14.69	16.94
80	11.86	14.44	17.44
100	12.08	14.73	17.84

Finally using Eq. (3.19) number of cycles to failure for all 15 cases are found and shown in Fig: 4.16. In Fig: 4.16, N represents number of cycles to failure.

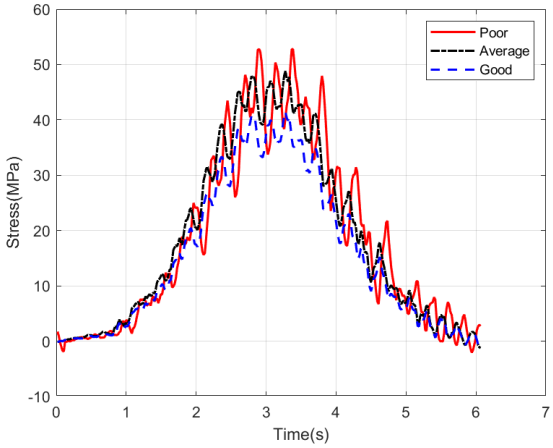

Fig: 4.11 Stress vs Time for three road conditions with Vehicle Velocity of 20 Kmph

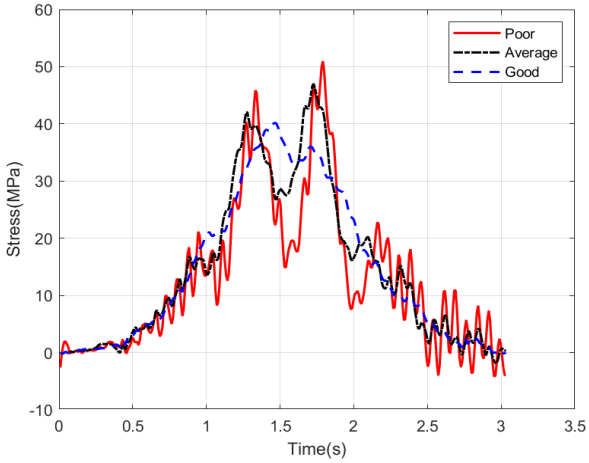

Fig: 4.12 Stress vs Time for three road conditions with Vehicle Velocity of 40 Kmph

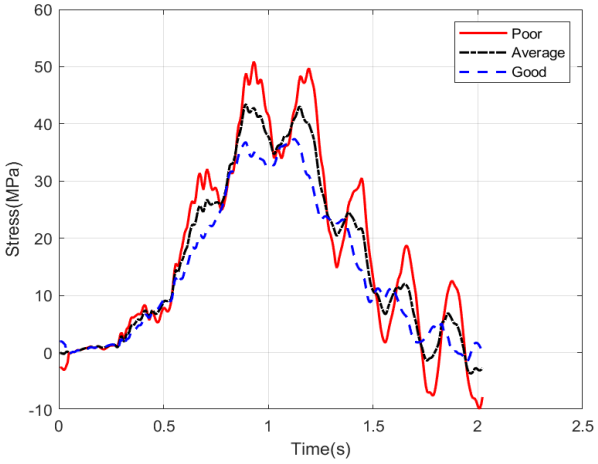

Fig: 4.13 Stress vs Time for three road conditions with Vehicle Velocity of 60 Kmph

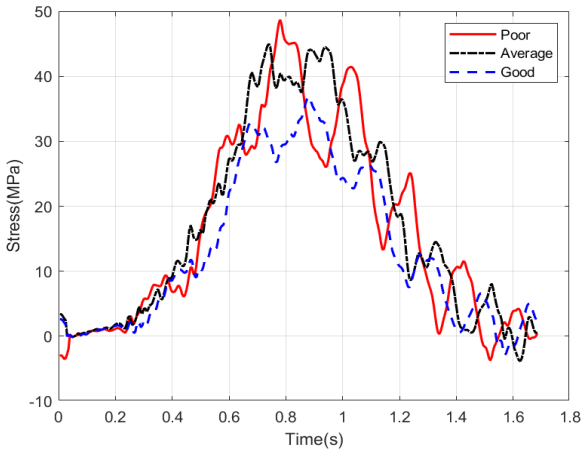

Fig: 4.14 Stress vs Time for three road conditions with Vehicle Velocity of 80 Kmph

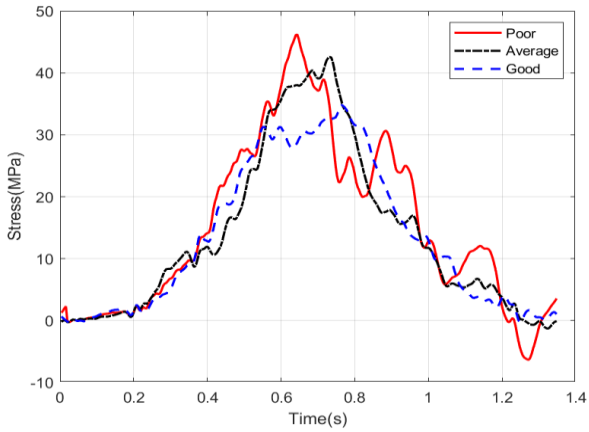

Fig: 4.15 Stress vs Time for three road conditions with Vehicle Velocity of 100 Kmph

From this study, it is found that, for velocity 20kmph, the fatigue life of bridge decreases by 48.78% when road surface condition degrades from good to average and by 33.93%

when road surface roughness degrades from average to poor. For other velocities, it is

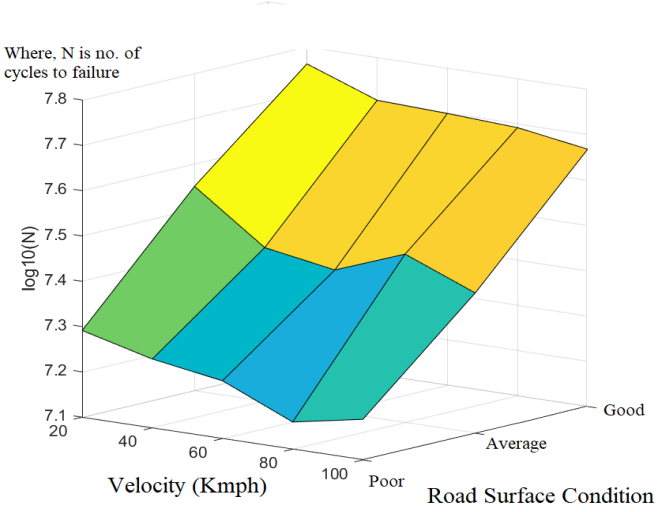

Fig: 4.16 Variation of fatigue life N with road surface condition and velocities

tabulated in Table 9 and represented in Fig: 4.16. From the results obtained, it is seen that, more deteriorated the road condition is, the more is the fatigue damage. The poor road condition has more dynamic impact on bridge inducing high stress range, hence reducing fatigue life of bridge. Various bridge (span, girder depth) and vehicle parameters (spring stiffness, mass etc.) affect the dynamic performance of bridge. Hence, in most cases, higher velocities induce larger stress range that results in smaller fatigue life but in some cases, it is seen that the fatigue life has increased while increase in velocity. Similar conclusions are drawn by various researchers (Zhang & Cai, 2012; Zhang, et al, 2013).

Table 9 Fatigue life (N) for different road surface condition and velocities

Velocity (kmph)	Fatigue Life (N)			% Difference of Fatigue Life (N)		
	Good	Average	Poor	Good to Average	Average to poor	
20	6.94E+07	3.55E+07	2.35E+07	48.78	33.93	
40	5.07E+07	2.75E+07	1.79E+07	45.83	34.99	
60	5.01E+07	2.59E+07	1.69E+07	48.3	34.79	
80	4.92E+07	2.67E+07	1.81E+07	45.8	32.24	
100	4.66E+07	2.57E+07	1.55E+07	44.84	39.75	

CHAPTER 5: CONCLUSIONS AND RECOMMENDATIONS

5.1 Conclusions

In this study, the fatigue life of existing steel-concrete composite bridge is calculated for good, average and poor road surface condition of bridge deck. The road surface roughness profile is generated using the guideline of ISO8608. Then, for three road surface conditions, the vehicle bridge interaction using iterative method is done to obtain stress time histories at the bridge girder. This stress time history contains variable amplitudes of stresses. These variable amplitude stresses are converted into constant amplitude stress by using rain flow cycle counting method. Then, equivalent constant amplitude stress range is obtained according to linear damage rule.

The study shows that, the fatigue life of bridge decreases by 48.78% when road surface condition degrades from good to average and by 33.93% when road surface roughness degrades from average to poor for 20kmph vehicle velocity. For velocity 40kmph, the fatigue life of the bridge decreases by 45.83% when road surface condition degrades from good to average and by 34.99% when road surface roughness degrades from average to poor. For velocity 60kmph, the fatigue life of the bridge decreases by 48.3% when road surface condition degrades from good to average and by 34.79% when road surface roughness degrades from average to poor. The fatigue life of bridge decreases by 48.80% when road surface condition degrades from good to average and by 32.24% when road surface roughness degrades from average to poor for 80kmph vehicle velocity. Similarly, the fatigue life of bridge decreases by 44.84% when road surface condition degrades from good to average and by 39.75% when road surface roughness degrades from average to poor for 80kmph vehicle velocity.

It can be concluded that, if we do not maintain the road surface in the bridge, as seen from this study, the bridge will fail due to fatigue. So, this study suggests that road surface in the bridge deck must be maintained so that bridge will have longer life.

The method used in this study can be applied to find out remaining fatigue life of the existing bridges if the existing crack size in the bridge girder is known. If the existing crack size i.e. initial crack size in the bridge girder can be measured, we can simply find the remaining fatigue life of that bridge by using Paris Law based on Linear Elastic Fracture Mechanics.

5.2 Recommendations for further Studies

In some cases, it is observed that the fatigue life has increased due to increase in velocity. This may be because of various parameters like vehicle mass, vehicle suspension; tire spring stiffness, bridge span length, girder dimensions, loading frequencies, etc. have effect on dynamic performance of vehicle and bridge. Further research is required to pin point the reason behind this result.

CHAPTER 6: REFERENCES

Albrecht, & Yazdani. (1986). Risk analysis extending the service life of the steel bridges. *Report FHWA/MD No. 84/01.*

Anderson, T. (2005). *Fracture mechanics: Fundamentals and applications.* 6000 Broken Sound Parkway NW: Taylor & Francis Group.

Barsom, J., & Rolfe, S. (1987). *Fracture and fatigue control in structures: applications of fracture mechanics.* West Conshohocken, PA: ASTM

Broek, D. (1988). *Practical use of fracture mechanics.* Dordrecht, The Netherlands: Kluwer Academic Publishers.

Cai, C., Shia, X., Araujo, M., & Chen, S. (2007). Effect of approach span condition on vehicle-induced dynamic response of slab-on-girder road bridges. *Engineering Structures, 29,* 3210-3226

Chatterjee, Datta, & Surana. (1994). Vibration of continuous bridges under moving vehicles. *Journal of Sound and Vibration, 169,* 619-632

Clough, R., & Penzien, J. (2015). *Dynamics of structures.* New Delhi, India: CBS Publishers and Distributors Pvt. Ltd.

Deng, L., & Cai, C. (2010). Development of dynamic impact factor for performance evaluation of existing multi-girder concrete bridges. *Engineering Structures, 32,* 21-31

Deng, L., Wang, W., & Cai, C. (2016). Effect of pavement maintenance cycle on the fatigue reliability of simply-supported steel I-girder bridges under dynamic vehicle loading. *Engineering Structures,133,*124-132.

Dodds, C. J., & Robson, J. D. (1973). The description of road surface roughness. *Journal of Sound and Vibration,31,* 175-183.

Endo, T., Mitsunaga, K., Takahashi, K., Kobayashi, K., & Matsuishi, M. (1974). Damage evaluation of metals for random or varying loading: three aspects of rain flow method. *Mechanical Behavior of Materials*, *1*, 371–380.

Feriani, A., Mulas, M. G., &Aliprandi, C. (2006). Time domain iterative procedures for vehicle-bridge dynamic interaction. *International Conference on Noise and Vibration Engineering,* 1179-1194

Fisher, J. (1984). *Fatigue and fracture in steel: case studies*. New York: John Wiley & Sons

Green, M., Cebon, D., & Cole, D. (1995). Effects of vehicle suspension design on dynamics of highway bridges. *Journal of Structural Engineering, 121(2),*272-282

Hawk, H., &Ghali, A. (1981). Dynamic response of bridges to multiple truck loading. *Canadian Journal of Civil Engineering, 8(3),* 392-401

Henchi, K., Fafard, M., Talbot, M., & Dhatt, G. (1998). An efficient algorithm for dynamic analysis of bridges under moving vehicles using a coupled modal and physical components approach. *Journal of Sound and Vibration, 212,* 663-683

Hirt, M., & Fisher, J. (1973). Fatigue crack growth in welded beams. *Engineering Fracture Mechanics, 5(2),* 415-429

Huang, Wang, & Shahawy. (1992). Impact analysis of continuous multi girder bridges due to moving vehicles. *Journal of Structural Engineering, 118(12),* 3427-3443

Huang, X., Zhuo, W., & Shang, G. (2014). Ansys-based spatial coupled vibration analysis method of vehicle-bridge interaction system. *Key Engineering Materials, 574,* 117-126

Hwang, & Nowak. (1992). Simulation of dynamic load for bridges. *Journal of Structural Engineering, 117(5),* 1413-1434

Kondo, Y. (N.D.). Fatigue under variable amplitude loading. *Cyclic Loading and Fatigue, 4,* 253-279

Leitão, F., Silva, J. d., & Andrade, S. d. (2013). Fatigue analysis and life prediction of composite highway bridge decks under traffic loading. *American Journal of Solids and Structures, 10(3),* 505-522

Li, H., & Wu, G. (2020). Fatigue evaluation of steel bridge details integrating multi-scale dynamic analysis of coupled train-track-bridge system and fracture mechanics. *Applied Science,10,* 3261

Liu, Y., Li, D., Zhang, Z., & Zhang, H. (2017). Fatigue load model using the weigh-in-motion system for highway bridges in China. *Journal of Bridge Engineering, 22(6)*

MacDougall, C., Green, M. F., & Shillinglaw, S. (2006). Fatigue damage of steel bridges due to dynamic vehicle loads. *Journal of bridge engineering, 11(3),* 320-328

Materials, A. S. (2001). Astm Standard E1049.

Miner. (1945). Cumulative damage in fatigue. *Journal of Applied Mechanics, 12,* A159-A164

Paris, P. C. (1961). A rational analytical theory of fatigue. *Trends Engineering, 13*

Pugno, N., Ciavarella, M., Cornetti, P., & Carpinteri, A. (2006). A generalized Paris' law for fatigue crack growth. *Journal of the Mechanics and Physics of Solids, 54,* 1333-1349.

R.Narayanan, &T.M.Roberts. (2005). *Structures subjected to repeated loading.* CRC Press

Robson, D. (1973). The description of road surface roughness. *Journal of sound and vibrations, 31,* 175-183

Shi, X., Cai, C. S., & Chen, S. (2015). Vehicle induced dynamic behavior of short-span slab bridges considering effect of approach slab condition. *Journal of Bridge Engineering,* 13(1), 83-92

Tada, H., & Irwin, G. R. (1975). K-value analysis for cracks in bridge structures. *Fritz Laboratory Reports*.

Wang, L., Jiang, P., Hui, Z., Ma, Y., Liu, K., & Kang, X. (2016). Vehicle-bridge coupled vibrations in different types of cable stayed bridges. *Frontiers of Structural and Civil Engineering, 10,* 81-92

Wang, L., Kang, X., & Jiang, P. (2015). vibration analysis of a multi-span continuous bridge subject to complex traffic loading and vehicle dynamic interaction. *KSCE Journal of Civil Engineering, 20,* 323-332

Wang, T., & Huang, D. (1992). Computer modeling analysis in bridge evaluation. *Interim Res. Report,* Florida Department of Transportation. Report No. FL/DOT/RMC/0542-3394, Tallahassee, Fla

Wang, F.-Y., Xu, Y.-L., Sun, B., & Zhu, Q. (2019). Dynamic stress analysis for fatigue damage prognosis of long-span bridges. *Structure and Infrastructure Engineering,* 1-18.

Yazdani, N., & Albrecht, P. (1990). Probabilistic fracture mechanics application to highway bridge. *Engineering Fracture Mechanics, 37(5),* 969-985

Yu, H., Wang, B., Li, Y., Zhang, Y., & Zhang, W. (2018). Road vehicle-bridge interaction considering varied vehicle speed based on convenient combination of Simulink and Ansys. *Shock and Vibration, 3,* 1-14

Zettlemoyer, N. (1976). Stress concentration and fatigue of welded details. Thesis, Lehigh University, Bethlehem, PA

Zettlemoyer, N., & Fiisher, J. W. (1978). Stress gradient and crack shape effects on stress intensity at welded details. *Welding Journal, 57(2),* 57-62

Zettlemoyer, N., & Fisher, J. W. (1977). Stress gradient correction factor for stress intensity at welded stiffeners and cover plates. *Welding Journal*, *56(12)*, 393-398

Zhang, W., & Cai, C. (2012). Fatigue reliability assessment for existing bridges considering vehicle speed and road surface conditions. *Journal of Bridge Engineering*, *17(3)*, 443-453

Zhao, Z., & Haldar, A. (1996). Bridge fatigue damage evaluation and updating using non-destructive inspections. *Engineering Fracture Mechanics, 53(5)*, 775-788

Zhao, Z., Haldar, A., & Breen, F. L. (1992). Fatigue-reliability updating through inspections of steel bridges. *Journal of Structural Engineering*, *120(5)*, 1624-1642

Zhao, Z., Haldar, A., & Jr, F. L. (1994). Fatigue reliability evaluation of steel bridges. *Journal of Structural Engineering, 120(5)*, 1608-1623